

# ECH and ECCD modelling studies for DTT

Benedetta Baiocchi<sup>1\*</sup>, Lorenzo Figini<sup>1</sup>, Alessandro Bruschi<sup>1</sup>, Francesco Fanale<sup>2</sup>, Saul Garavaglia<sup>1</sup>, Gustavo Granucci<sup>1</sup>, and Afra Romano<sup>2,3</sup>

<sup>1</sup>Institute for Plasma Science and Technology – CNR, via Cozzi 53, 20125 Milano, Italy

<sup>2</sup>EDP ENEA, Fusion and Nuclear Safety Department, C. R. Frascati, via E. Fermi 45 00044, Frascati, Italy

<sup>3</sup>DTT S.c. a r.l., C. R. Frascati, via E. Fermi 45 00044, Frascati, Italy

**Abstract.** In this work the Electron Cyclotron (EC) physics performances of the EC system foreseen for the new Divertor Tokamak Test facility (DTT) are investigated using the beam tracing code GRAY on the flat top phase of the most recent DTT full power scenario. The whole core plasma region can be reached by EC beams with complete absorption, assuring bulk heating and core current drive (CD) for profile tailoring, and NTM mitigation in correspondence of the rational surfaces. A detailed analysis regarding modifications of the EC propagation, absorption and CD location due to density fluctuations caused by pellet injection is performed. The compatibility between the EC system and the pellet injection system is verified: the density variations due to pellet injection are foreseen to negligibly influence the EC performances, allowing the EC beams to reach the plasma central region for bulk heating and to drive current on the rational surfaces for NTM mitigation. Finally, the polarization variations originated by the angle steering foreseen for the operational and physics tasks accomplishment during the flat top phase of the discharge are assessed. Negligible power losses have been found keeping fixed polarization during the needed steering.

## 1 Introduction

The new Divertor Tokamak Test facility (DTT [1]), aimed to perform studies regarding power exhaust and divertor load and currently under construction, will be provided with a mix of additional heating systems. The electron cyclotron (EC) system is foreseen to be the main heating system. It will contribute to assure high power flow, and it has the aim of accomplishing several operational and physics tasks: plasma current ramp-up & ramp down, L- to H-mode transition, core heating & current drive (CD), control of MHD modes as sawteeth (ST) and neoclassical tearing modes (NTM), plasma current density and electron temperature profile tailoring, mitigation of impurity accumulation and wall cleaning. Then proper different radial localizations and combination of heating and non-inductive current drive must be provided, taking into account the peculiar physics requirements and the engineering constraints of such new machine. To this purpose, two types of launcher have been proposed [2,3]: two different antennas are foreseen to be hosted in the equatorial and in the upper port of each ECRH sector, with 6 and 2 single launchers respectively. The 8 launchers of a cluster are independently steerable to improve the flexibility, allowing EC absorption over a broad range of plasma locations. In order to investigate and to optimize launchers performances for the foreseen EC tasks, the beam-tracing code GRAY [4] has been used

to perform a comprehensive study regarding the propagation, absorption and current drive of the EC beams, as reported in Section 1. Such study has been applied to the flat top phase of the reference DTT Single Null full power scenario [5], characterized by  $B_T=5.85$  T,  $I_p=5.5$  MA,  $R=2.19$  m,  $a=0.7$  m, by additional power coupled to the plasma  $P_{add}=45$  MW (28.8 MW from EC), and by the kinetic profiles reported in fig. 1-left. Fig. 1-right shows the main baseline scenario equilibrium features (the poloidal projection of the flux surfaces, with rational surfaces represented with green lines) and the EC launcher parameters, i.e. the resonance layer in the plasma correspondent to the selected frequency of 170 GHz, and examples of the beams paths launched from the Upper and from the top and bottom Equatorial ports launcher positions.

Then sensitivity studies regarding the EC performances variation have been carried out, considering the characteristics of the DTT full power scenario which can be critical for proper EC system operation. As shown in fig. 1-left, the reference DTT full power scenario is characterized by high density plasma ( $n_{e0}\sim 2.5e20$  m<sup>-3</sup>, which means a plasma frequency  $f_p\sim 142$  GHz), requiring then pellet injection as fuelling system [5]. Perturbations due to pellet injection on high density profiles can imply high beam refraction and then issues can rise regarding beam localization in correspondence of the rational surfaces, which are externally located in the considered scenario (see fig. 1-right). Section 2

\* Corresponding author: [benedetta.baiocchi@istp.cnr.it](mailto:benedetta.baiocchi@istp.cnr.it)

reports evaluations regarding EC beam propagation deviations and (if needed) steering corrections for the DTT full power scenario with injection of pellets with different sizes. In order to fulfill all the physics tasks foreseen for the EC system during the plasma discharge, wide angles steering is required. The correct injected beam polarization has to be preserved for achieving an optimal coupling to Ordinary mode when operating at the first harmonic resonance, as foreseen for the full power DTT scenario. A detailed investigation of polarization variation due to angles steering is reported in Section 3. Finally, a short summary follows in Section 4.

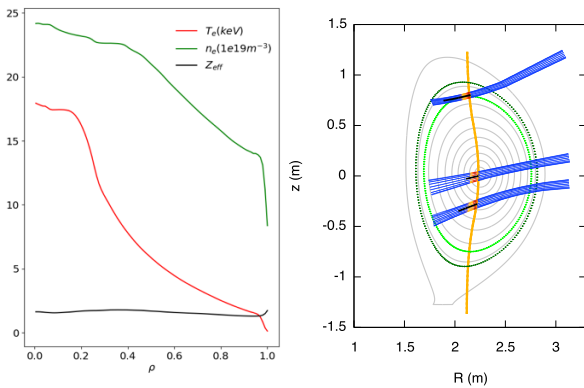


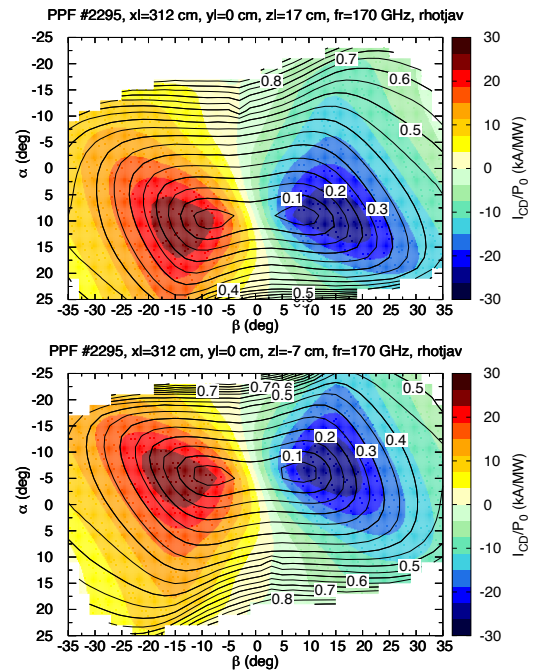
**Fig. 1.** (left) Electron density (green), electron temperature (red) and effective  $Z$  (black, with average  $Z_{eff}\sim 1.6$ ) profiles of the DTT full power scenario, used as input in beam tracing simulations.  $\rho$  is calculated as the squared root of the normalized toroidal flux. (right) Poloidal projection of the flux surfaces and of the path of different EC beams varying the launching position/angles. In yellow the resonance layer for 170 GHz. In (dark) green the poloidal projection of the  $q=3/2$  ( $q=2/1$ ) surface, located at  $\rho=0.701$  ( $\rho=0.814$ ).

## 2 EC propagation, absorption and CD analysis

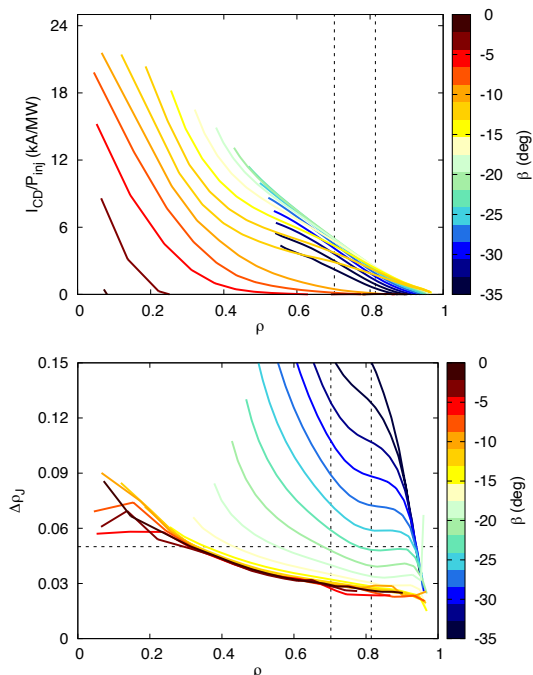
In order to investigate and to optimize the EC performances, parametric studies have been performed, varying the injection angles ( $\alpha$ =poloidal,  $\beta$ =toroidal), considering the DTT full power scenario reported in fig.1 and the EC launcher specifications as [2] (injection frequency of 170 GHz in Ordinary mode, and 3 launcher positions: top and bottom equatorial (EQT, EQB), and upper (UP)).

Fig. 2 shows the driven current per unit of injected power with varying  $\alpha$  and  $\beta$ , for the top and bottom equatorial launchers. Complete absorption is found for large angles intervals, narrower limits are given by engineering constraints [3]. The allowed ranges of angles ( $-10^\circ < \alpha < 25^\circ$  for EQT,  $-25^\circ < \alpha < 10^\circ$  for EQB,  $-25^\circ < \beta < 25^\circ$ ) permit to reach the plasma in the central region ( $\rho\sim 0.1$ ) as the peripheral core plasma ( $\rho < -0.7-0.8$ ).  $\beta < 0$  gives co-driven current, with the maximum value of 25 kA/MW in correspondence of  $\rho\sim 0.1$ . Core heating and CD are well performed by equatorial launchers, then allowing the accomplishment of the task of bulk heating. Such results are promising also in order to achieve the additional tasks of profile tailoring and

sawteeth instabilities stabilization. Very recently, theoretical studies and integrate modelling works have been started to perform a detailed analysis of the quantitative requirements for EC to fulfill such tasks in the most recent reference full power DTT scenario [6]. For NTM mitigation, which is carried out by driving current in correspondence of the rational surfaces  $q=3/2$  and  $q=2$ , the Upper launcher is preferable for launching geometry.



**Fig. 2.** Calculated driven current per unit power for the top (top) and bottom (bottom) equatorial launchers with varying poloidal ( $\alpha$ ) and toroidal ( $\beta$ ) angles. Driven current average location is represented by black contours.



**Fig. 3.** (top) Calculated driven current per unit power and (bottom) average current density profile width as functions of the driven current average location. Colours refer to different  $\beta$  values. Every point of every line corresponds to a different

$\alpha$  value ( $10^\circ$ - $50^\circ$ ). Locations of the rational  $q$  surfaces ( $\rho=0.701$  for  $q=3/2$  and  $\rho=0.814$  for  $q=2$ ) are shown by vertical dashed black lines. The horizontal dashed line in figure on the bottom represents the value  $\Delta\rho=0.05$

Fig. 3 shows the driven current per unit of injected power and the width of the relative current density profiles as function of the driven current average location, with varying  $\alpha$  and  $\beta$ , and launching from the upper position. The access to the plasma in the internal core region ( $\rho<0.4$ ) is reached for  $|\beta|<15^\circ$ . In the outer core region, where  $q=3/2$  and  $q=2$  are located, the maximum value of the driven current per unit of injected power is obtained for  $|\beta|$  between  $20^\circ$  and  $22^\circ$ , obtaining  $I_{cd}/P_0\sim 5$  kA/MW for  $q=3/2$  and  $I_{cd}/P_0\sim 2.5$  kA/MW for  $q=2$ . The narrower current density profile is found for the minimum  $|\beta|$  of such interval, ( $|\beta|=20^\circ$ ), and it satisfies  $\Delta\rho\leq 0.05$  (i.e.  $\sim 3.5$  cm when measured at the plasma midplane), which is the expected requirement for NTM control for DTT [1].

### 3 EC analysis in presence of density fluctuation due to pellets injection

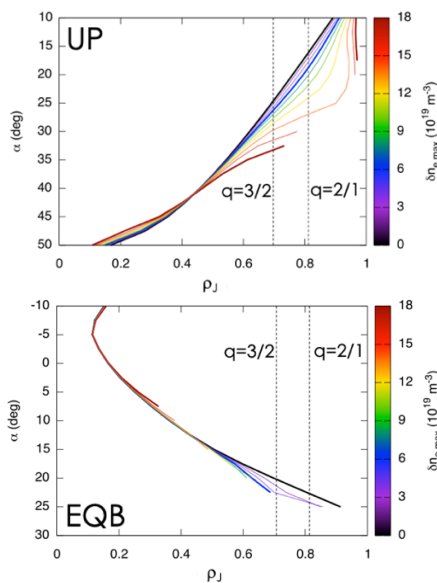


**Fig. 4.** Poloidal angles  $\alpha$  and relative current density average location for upper (top: with toroidal angle  $\beta=15^\circ$ ) and bottom equatorial launchers (bottom: with toroidal angle  $\beta=5^\circ$ ). Colours refer to different density perturbation amplitude. Location of the rational  $q$  surfaces are shown by vertical dashed black lines.

Among the particle fuelling methods, the pellets injection system has been foreseen for DTT. In order to evaluate the compatibility of the EC system with the density fluctuations due to pellet injection, first an analysis regarding the maximum allowed density perturbation has been performed. We have considered as Gaussian perturbation a Gaussian deposition profile given by  $\delta n_e(\rho)\sim\delta n_{e,max}\exp[-(\rho-\rho_{dep})^2/(2\Delta\rho_{dep}^2)]$ , where  $\rho_{dep}=0.8$  is the central location,  $\Delta\rho_{dep}=0.09$  is the width at half height, and  $\delta n_{e,max}$  is the amplitude of the considered perturbation. The full power scenario density profiles with adding the above described density

perturbation have been used as GRAY inputs, with adjusting the temperature profiles in order to have a constant pressure profile. The analysis performed with varying the amplitude of the density perturbation gives the results shown in fig. 4. Higher values of the perturbation density could cause strong beam refraction, and then the reduction of available poloidal steering range, which, as shown in fig. 4, does not cover anymore the whole core region with complete absorption. Regarding the upper launcher performances, the beam is not negligibly affected for  $\delta n_{e,max}>6e19 m^{-3}$ , and even large angle adjustments ( $2^\circ$ - $20^\circ$ ) can be required for off-axis aiming, i.e. to reach the rational surfaces. The core is still reachable despite large density perturbations. However the prediction and the control of the power deposition and the ECCD location could be scarcely reliable.

After such analysis, which gives general indication about the EC compatibility with density perturbations in the peripheral plasma core for the DTT full power scenario, a detailed investigation has been performed with the GRAY code, using as input the kinetic profiles and the equilibrium data of the time-dependent full power DTT scenario simulations [7]. They have been modelled with the JETTO transport code [8]: the pellet ablation and deposition have been predicted by the code HPI2 [9], which has been used self-consistently with the code suite. QuaLiKiz [10] has been used as transport model, while the ECRH has been prescribed. Although the current DTT reference configuration is based on a plasma radius equal to  $R=2.19$  m, without loss of significance the time-dependent simulations, and then the analysis here illustrated, have been carried out on a previous configuration characterized by  $R=2.14$  m.

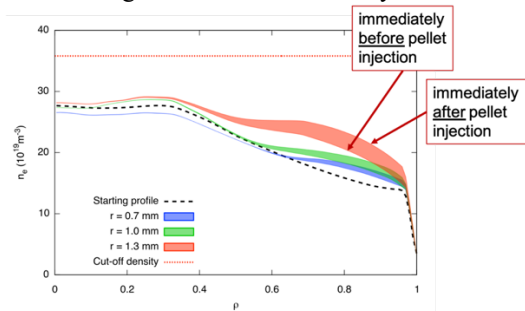


**Fig. 5.** Density profiles of the JINTRAC simulations without (dashed) and with pellets (coloured: blue for radius of 0.7 mm, green for 1 mm, red for 1.3 mm). The bottom and top sides of every band represent the profile immediately before and after one pellet injection. Density cut-off for Ordinary mode is represented by red dashed line.

The pellet injection geometry (oblique high field side) and the reference pellet parameters (radius 1 mm and velocity 516 m/s) have been chosen according to the previous DTT pellet injection modelling work performed with stand-alone HPI2 [11]. The pellet frequency injection (16 Hz) has been selected in order to sustain the desired density pedestal. Fig. 5 shows the resulting density profiles of the time-dependent simulations using the reference pellet parameters (green), and two realistic variations reported in [11] (blue: radius=0.7 mm, red: radius=1.3 mm). The lower and the higher sides of every colored band represent the

density profile just before and just after the pellet injection for every ‘pellet cycle’ in stationary conditions. The dashed line represents the starting density profile of the time-dependent simulations, and it has been obtained using gas puffing as fuelling method. The density perturbation due to pellet ablation can involve a broad region of the plasma ( $0.4 \leq \rho \leq 0.95$ ). The perturbed density profile keeps lower values than the Ordinary mode density cut-off for all the considered cases. The local density increase compared to the initial profile which spans from  $\delta n_{e,max}=1e19 \text{ m}^{-3}$  (15%) to  $\delta n_{e,max}=7e19 \text{ m}^{-3}$  (40%) depending on the pellet dimensions. However, in all the cases, the variation of the density values between two consecutive pellets does not exceed 10%.

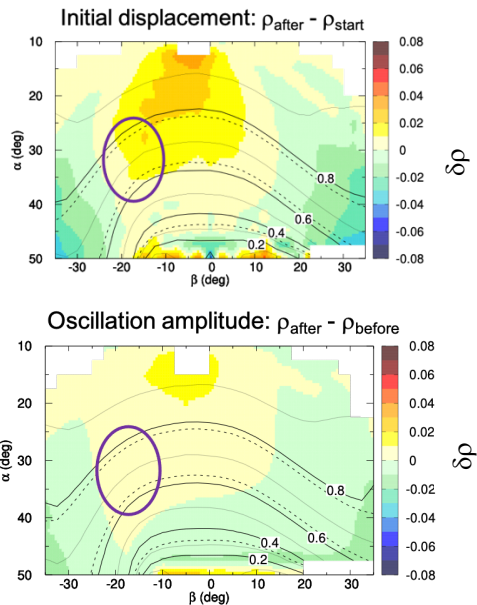
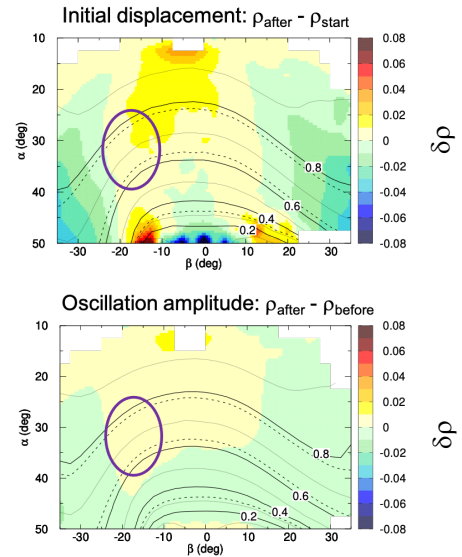


**Fig. 6.** Displacement  $\delta\rho$  of the ECCD location due to pellets  $n_e$  modifications by varying toroidal and poloidal angles for reference pellets (1 mm) (top: between the case just after pellet and without pellet, bottom: between the case just after pellet and just before pellet). Black contours: reference ECCD location (before pellet injection). Dashed lines represent the rational  $q$  surfaces for the DTT full power scenario ( $R=2.14 \text{ m}$  configuration). Violet ellipse highlights the optimized intervals of injection angles which reach the rational  $q$  surfaces 2 and  $3/2$ .

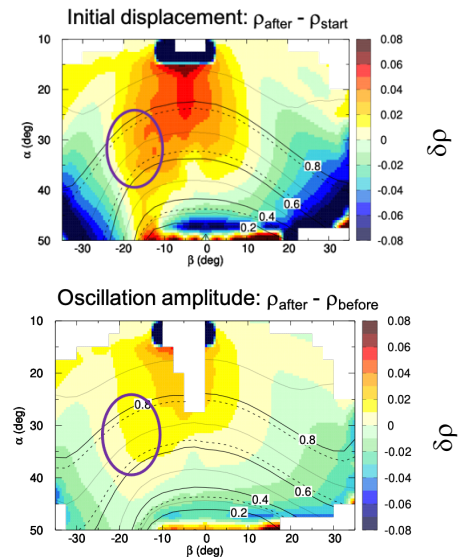
In order to investigate in detail the effects that these more realistic density profiles variations due to pellet injection have on EC propagation, absorption and CD, stand-alone GRAY simulations have been performed varying the injection angles and using as input the profiles of the different phases of the pellet cycle. We limit the analysis to the upper launcher case, because, as it has been found from the initial investigation regarding the maximum allowed perturbation, the inner region of the plasma core is reached even in presence of large density deviation.

Fig. 6 shows the radial displacement of the ECCD location due to density modifications induced by pellets for the reference case of radius=1 mm. With respect to the case without pellets, the radial deviation in correspondence of the location of the rational surfaces reached by the optimized injection angles (see Section

1) is  $\delta\rho \sim 0.02$ , and  $\delta\rho < 0.02$  during a pellet cycle. Such displacement is lower than the width of the current density profile, then it should not require any adjustment of the steering angles.



**Fig. 7.** Displacement  $\delta\rho$  of the ECCD location due to  $n_e$  modifications due by pellets varying toroidal and poloidal angles for pellets of 0.7 mm (top: between the case just after pellet and without pellet, bottom: between the case just after pellet and just before pellet). Black contours: reference ECCD location (before pellet injection). Dashed lines represent the rational  $q$  surfaces ( $R=2.14 \text{ m}$  configuration). Violet ellipse highlights the optimized intervals of injection angles which reach the rational  $q$  surfaces 2 and  $3/2$ .



**Fig. 8.** Displacement  $\delta\rho$  of the ECCD location due to  $n_e$  modifications due by pellets varying toroidal and poloidal angles for pellets of 1.3 mm (top: between the case just after pellet and without pellet, bottom: between the case just after pellet and just before pellet). Black contours: reference ECCD location (before pellet injection). Dashed lines represent the rational  $q$  surfaces ( $R=2.14 \text{ m}$  configuration). Violet ellipse highlights the optimized intervals of injection angles which reach the rational  $q$  surfaces 2 and  $3/2$ .

As fig. 7 shows, in the case with pellets of radius 0.7 mm the deviation is almost negligible. The radial displacement for larger pellets can instead require some

modification: for pellets with radius=1.3 mm (see fig. 8) the radial deviation with respect to the case with no pellets reaches values  $\delta\rho\sim 0.04$  for the optimized angles for NTM control, while in a pellet cycle it is  $\delta\rho\sim 0.02$ .  $\delta\rho=0.04$  is comparable to the ECCD profile width, then, in order to correctly localize the current on the rational surfaces, a modification of the poloidal angle of  $2^\circ$  is needed. We can conclude that, for realistic pellet sizes, the ‘real-time’ corrections of the steering angles during the plasma discharge, if needed, are of the order of the degree. The density variations due to pellet injection as predicted by HPI2 are then highly lower with respect to the values which prevent the EC beams reaching the outer plasma region (see Fig. 4). Such perturbations are then foreseen not really problematic for EC performances in realistic DTT scenarios.

## 4 Polarization analysis

In order to couple the EC launched wave to the desired mode in the plasma, the wave polarization must be properly imposed by the launcher. However, incident wave ellipticity ( $\chi$ ) and ellipse inclination ( $\psi$ ), which characterize the polarization, depend respectively on the magnitude of the magnetic field and the angle of incidence, and on the magnetic pitch angle at the plasma boundary. The angles steering, which could be needed during the plasma discharge for the achievement of the operational tasks, can have a not negligible effect on the ellipticity and the ellipse inclination, requiring to consequently adjust the injected wave polarization. Fig. 9 shows the values obtained for ellipticity and ellipse inclination varying the steering angles for the upper launcher. As expected, larger changes of the ellipticity are due to toroidal angle variation, while the ellipse orientation depends both by toroidal and poloidal steering.

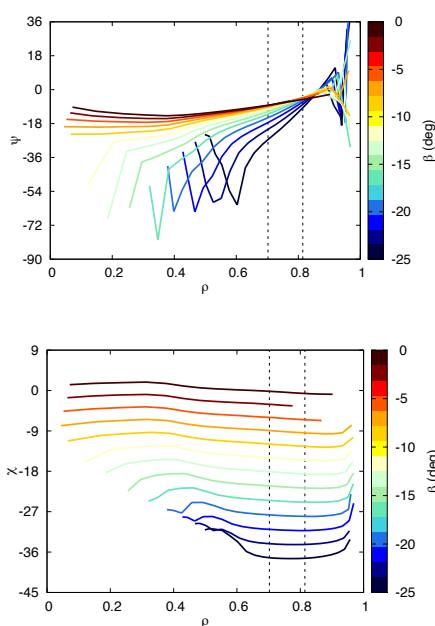


**Fig. 9.** (top)  $\psi$  and (bottom)  $\chi$  as functions of the average current density location. Colours refer to different  $\beta$  values. Every point of every line corresponds to a different  $\alpha$  value

( $10^\circ$ - $50^\circ$ ). Location of the rational  $q$  surfaces are shown by vertical dashed black lines.

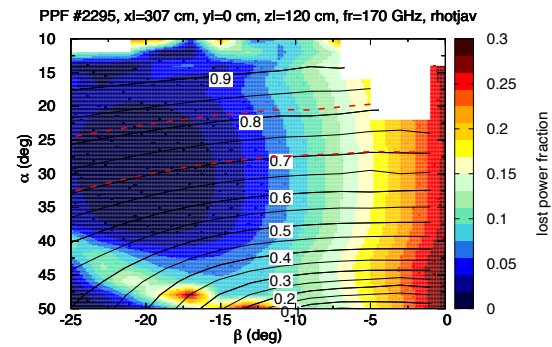


**Fig 10.** Lost power fraction using optimal  $\psi$  and  $\chi$  for  $q=3/2$  for the upper launcher, varying toroidal and poloidal angles. Red dashed lines represent the rational surfaces locations.

An estimate of the power which could be lost during the angle steering, if the polarizer is not properly adjusted, is shown in Fig. 10. It has performed using as antenna polarizer parameters the optimal values for a selected angle couple ( $\alpha=30^\circ$ ,  $\beta=-20^\circ$ , for reaching the rational surface  $q=3/2$ ) and calculating for every other couple of angles the power which is not coupled to the ordinary mode. Considering the couple of angles reaching the rational surface  $q=2$  ( $\alpha=23^\circ$ ,  $\beta=-20^\circ$ ), the fraction of lost power is very low, nearly 0.7%. The same analysis has been performed using as reference for the antenna polarizer parameters the ellipticity and the ellipse direction values of the couples of angles reaching  $q=2$  in the case without pellets ( $\alpha=28^\circ$ ,  $\beta=-20^\circ$ ). Without variations of the reference polarization values, the lost power calculated for the couples of angles reaching  $q=2$  for the cases with pellets is less than 0.6%, considering both profiles at the two sides of the pellet cycle.

## 5 Summary

The physics performances of the EC system have been investigated for the DTT reference full power scenario with the beam tracing code GRAY. The accessibility to the whole plasma core region with complete absorption is assured by both Equatorial and Upper EC launchers, with maximum current drive efficiency of 25 kA/MW located in  $\rho\sim 0.1$ . Regarding the optimization analysis for reaching the rational surfaces  $q=3/2$  and  $q=2$ , the best compromise between maximum CD and enough narrow current density profile has been found for the toroidal angle  $\beta=20^\circ$ .

The impact of pellet deposition perturbation on EC beam propagation has been studied, and EC performances have been assessed in time-dependent scenarios with pellet injection. The inner plasma core is always reached without any noticeable deviation, although lower prediction reliability is expected. In the region of the rational surfaces, for realistic pellets, the radial deviation of the EC localization with respect to the case without pellet profiles requires a maximum poloidal angle correction of few degrees. However, if the density profiles corresponding to the initial and final time of a pellet cycle are considered, no corrections are

required. Then the compatibility between the EC system and the pellet injection system has been verified for DTT. Additional calculations are needed to check such results for the time-dependent simulations of the DTT full power scenario with the present configuration  $R=2.19$  m, however similar conclusions are expected. Finally, the investigation of the wave polarization modifications due to injection angles steering has been performed. For the angle steering required for typical foreseen aims (i.e. sweeping between rational surfaces locations, or pointing the same rational surface during pellet injection) the power which is not be coupled with the ordinary mode has been found negligible.

The studies here reported have been performed on the flat-top of the reference DTT full-power scenario. As future work, the performances and optimization analysis is going to be focused on the dynamical phases of the DTT scenarios.

1. R. Martone *et al*, DTT Divertor Tokamak Test facility. Interim Design Report, ENEA (ISBN 978-88-8286-378-4), April 2019 ("Green Book")
2. S. Garavaglia *et al*, FED, 168, 112678 (2021)
3. A. Romano *et al*, Poster 1.17 at this conference
4. D. Farina, *et al*, Fusion Sci. Tech. **52**, 154 (2007)
5. I. Casiraghi, *et al*, Nucl. Fusion **61**, 116068 (2021)
6. I. Casiraghi *et al*, 48th EPS Conference on Plasma Physics (Virtual Edition, June 27-July 1 2022), O2.108
7. B. Baiocchi *et al*, to be submitted to Nucl. Fusion
8. G. Cenacchi *et al* *JETTO: A Free-boundary Plasma Transport Code* (JET Joint Undertaking, 1988)
9. B. Pegourie' *et al* Nucl. Fusion 47 44, (2006)
10. C. Bourdelle *et al* Phys. Plasmas 14, 112501 (2007)
11. B.Pégourié and E.Geulin, 2020 Final Report of EFDA\_D\_2PEJWH - PMI-2.3-T011-D001 EXTRA - Common milestones PEX/DTT, Topic 4: - CEA-01 Neutrals and impurities model and pumping <http://idm.euro-fusion.org/?uid=2PEJWH>